

Supplementary information

Tailoring MIL-100(Fe)-derived Catalyst for Controlled Carbon Dioxide Conversion and Product Selectivity

Hany E. Ahmed^{1,2,3a}, Mohamed
K. Albolkany^{4,b*}, Mohamed E. El-Khouly^{1,c}, Ahmed Abd El-Moneim^{1,3,5d*}

¹ Nanoscience Program, Institute of Basic and Applied Sciences, Egypt-Japan University of Science and Technology, New Borg El-Arab city, Alexandria 21934, Egypt.

² National Institute of Standards, Tersa St, El-Matbah, Haram, P. O. Box: 136, Code No 12211 Giza, Egypt.

³ Graphene Center of Excellence, Energy and Electronics Applications, Egypt-Japan University of Science and Technology, New Borg El-Arab, 21934, Egypt.

⁴ Department of Environmental Studies, Institute of Graduate Studies and Research, Alexandria University, Alexandria, Egypt.

⁵ Physical Chemistry Department, National Research Centre, El-Dokki, Cairo, 12622, Egypt.

^ahany.elmenyawi@ejust.edu.eg,

^bmohamed.masoud@alexu.edu.eg, ^cmohamed.elkhouly@ejust.edu.eg,

^dahmed.abdelmoneim@ejust.edu.eg.

*(Corresponding author)

Keywords: Carbon dioxide hydrogenation; Particle size effect; Iron-based catalyst; Metal-organic frameworks.

1. Supplementary figures

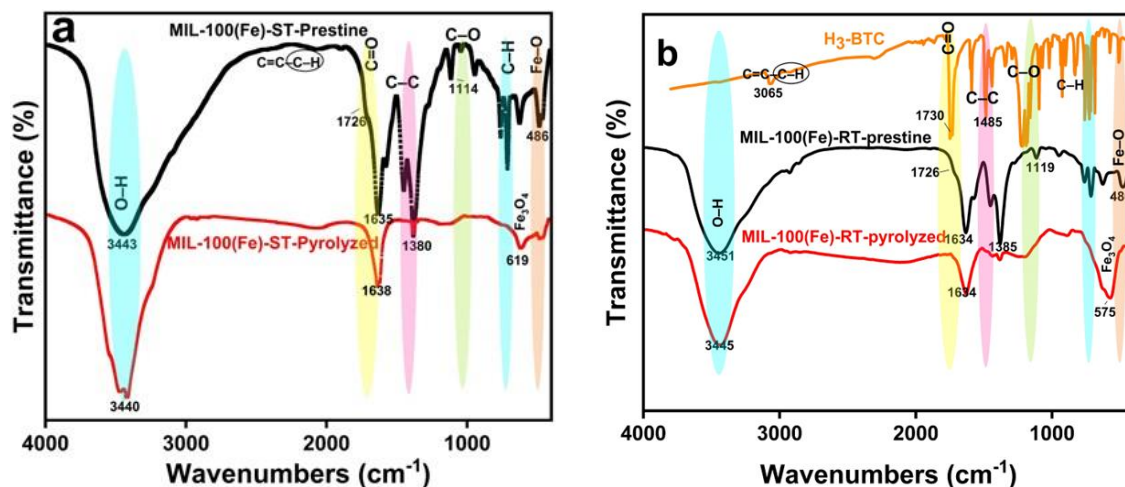


Fig. S1. FTIR spectra of a) pristine and pyrolyzed ST-based-MIL-100(Fe), and b) trimesic acid, pristine, and pyrolyzed RT-based-MIL-100(Fe).

The coordination between iron ions (Fe^{+3}) and the H_3BTC linker is characterized by a robust affinity, leading to a discernible reduction in the intensity of the characteristic bands attributed to H_3BTC ¹. The benzene ring demonstrates vibrational modes of in-plane and out-of-plane bending and stretching, with respective frequencies of 1453, 1119, and 770 cm^{-1} . Also, the vibrations of the carbonyl group of trimesic acid at 1730 cm^{-1} have weakened strongly due to the coordination effect and a new peak appeared in the range from 1300 to 1700 cm^{-1} related to the carboxylate group symmetrical and asymmetrical vibrations changes¹. Furthermore, there are discernible Fe-O bands that can be detected at frequencies of 631 and 475 cm^{-1} ². After pyrolysis, the carboxylate vibrations in the range from 1300 to 1700 cm^{-1} disappeared and the remaining vibrations at 1638 and 1634 cm^{-1} in case of ST- and RT-based catalysts, respectively, are attributed to the C=C vibrations in the carbon framework.

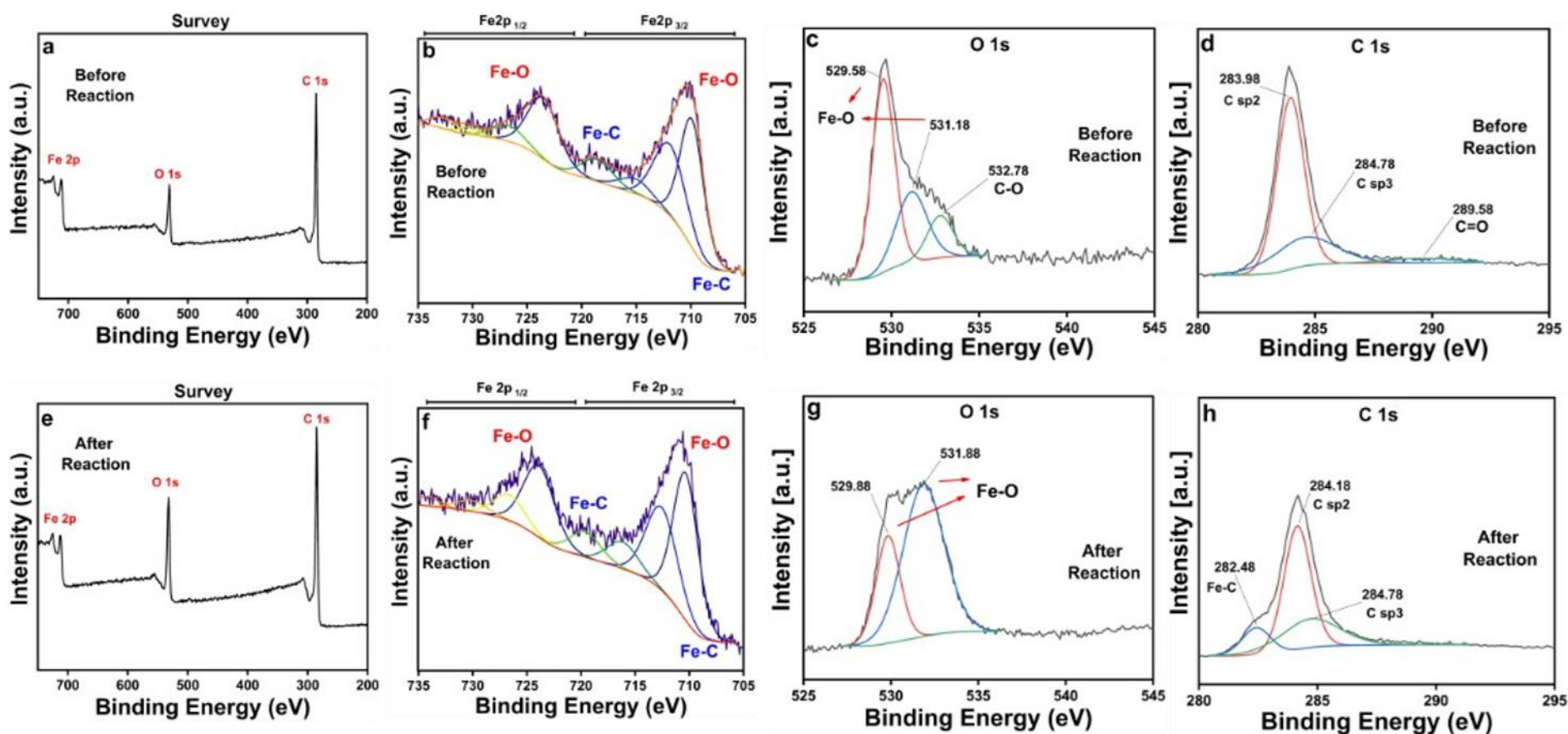


Fig. S2. XPS survey spectra before (a) and after (e) reaction, high-resolution Fe 2p spectra before (b) and after reaction (f), high-resolution O 1s spectrum before (c) and after reaction (g), and high-resolution C 1s spectrum before (d) and after reaction (h).

XPS analysis on the catalyst before (after treatment in CO: H₂ (2:1) gas mixture to prepare active phase (iron carbide and oxide)) and after the reaction was done. The survey spectrum before and after catalysis in **Fig. S2 (a and e)** illustrates that it comprises three elements: Fe, O, and C. The high resolution of Fe spectra (**Fig. S2 (b, f)**) shows two peaks at 708 and 720 eV which are attributed to iron carbides³. The peaks seen at 712.6 and 710.6 eV correspond to Fe(III) and Fe(II) 2p_{3/2}, respectively. The peaks at 726 and 724 eV are attributed to Fe(III) and Fe(II) 2p_{1/2}, respectively⁴. The peak ratio of FeC_x/FeO_x dropped slightly following the reaction without reducing catalytic activity, as demonstrated by the stability test in **Fig. 4(c)**. The high-resolution spectra of O 1s before the reaction show a 532.78 eV peak referred to C-O bond which remains from MOF structure after pyrolysis. This peak was removed after the reaction due to reduction by hydrogen and the feed gas. The peaks at 529 and 531 eV correspond to the Fe-O in magnetite. The high-resolution C 1s spectrum before the reaction also shows a peak at 289.5 eV, which indicates the presence of C=O remaining from the MOF structure⁵. The peak at 282.5 eV on the C 1s spectrum after the reaction is attributed to the Fe-C. The peaks at 284 and 284.8 eV match the Sp² and Sp³ carbon, respectively.

2. Supplementary tables

Table S1. The crystal size of MIL-100(Fe) prepared at room temperature and solvothermal and pore properties of the derived catalysts.

| <i>Sample</i> | Average crystal size of MIL-100(Fe) via TEM (nm) | Fe nanoparticles average size via TEM (nm) | $A_{s,BET}^a$ (m^2g^{-1}) | V_{total}^b (cm^3g^{-1}) | D_{mean}^c (nm) |
|--------------------------|--|--|-------------------------------|--------------------------------|-------------------|
| <i>RT-based catalyst</i> | 210 | 3 | 204 | 0.4 | 7.74 |
| <i>ST-based catalyst</i> | 249 | 10 | 54 | 0.2 | 15.3 |

^a specific BET surface area. ^b Total pore volume at ($\frac{P}{P_0} = 0.999$). ^c Mean pore diameter according to BJH method.

Table S2. H₂ consumption for pyrolyzed catalyst by TPR, and H₂ and CO₂ chemisorption on reduced catalyst by TPD.

| <i>Sample</i> | H ₂ consumption (mmole g ⁻¹) Pyrolyzed catalyst | H ₂ Uptake (mmole g ⁻¹) Reduced catalyst | CO ₂ Uptake (mmole g ⁻¹) Reduced catalyst | Normalized H ₂ -TPD peak area | Normalized CO ₂ -TPD peak area |
|--------------------------|---|--|---|--|---|
| <i>RT-based catalyst</i> | 0.268 | 4.320 | 0.898 | 1 | 0.699 |
| <i>ST-based catalyst</i> | 0.184 | 3.625 | 1.285 | 0.839 | 1 |

3. Supplementary equations

$$CH_4 \text{ Selectivity} = \frac{CH_4 \text{ outlet}}{\sum C_n H_m \text{ outlet}} \times 100\%$$

$$C_2-C_4 \text{ Selectivity} = \frac{\sum_2^4 C_n H_m \text{ outlet}}{\sum_1^n C_n H_m \text{ outlet}} \times 100\%$$

$$C_{5+} \text{ Selectivity} = \frac{\sum_5^n C_n H_m \text{ outlet}}{\sum_1^n C_n H_m \text{ outlet}} \times 100\%$$

4. References

1. E. Borfecchia, S. Maurelli, D. Gianolio, E. Groppo, M. Chiesa, F. Bonino, C. Lamberti, *J. Phys. Chem. C*, 2012, 116, 19839–19850.
2. H. Namduri and S. Nasrazadani, *Corros. Sci.*, 2008, 50, 2493–2497.
3. J. Chen, S. Ju, H. Park, K. Nasriddinov, C. Zhang, K. Jun, S. Kim, *Appl. Catal. B Environ.* 2023, 325, 122370.
4. A. Ramirez, L. Gevers, A. Bavykina, S. Ould-Chikh and J. Gascon, *ACS Catal.*, 2018, 8, 9174–9182.
5. B. Yao, T. Xiao, O. A. Makgae, X. Jie, S. Gonzalez-Cortes, S. Guan, A. I. Kirkland, J. R. Dilworth, H. A. Al-Megren, S. M. Alshihri, P. J. Dobson, G. P. Owen, J. M. Thomas and P. P. Edwards, *Nat. Commun.*, 2020, 11, 6395.